European Journal of Mechanics B/Fluids 28 (2009) 309–320

Contents lists available at ScienceDirect

European Journal of Mechanics B/Fluids

www.elsevier.com/locate/ejmflu

An experimental study of pulsating turbulent flow in a pipe

S. He [a,*], J.D. Jackson [b]

[a] *School of Engineering, University of Aberdeen, Aberdeen AB24 3UE, UK*
[b] *Simon Building, Oxford Road, University of Manchester, Manchester M13 9PL, UK*

ARTICLE INFO

Article history:
Received 27 July 2007
Received in revised form 13 May 2008
Accepted 22 May 2008
Available online 3 June 2008

Keywords:
Unsteady
Pulsating
Turbulent
Flow
Experimental
Pipe

ABSTRACT

An experimental study of pulsating turbulent flow in a pipe is reported in which measurements of instantaneous velocity were made using a two-component Laser Doppler Anemometer system. Local values of ensemble-averaged axial velocity, and radial and axial components of root-mean-square turbulent velocity fluctuation were obtained from the measurements. The frequency of the imposed pulsation of flow rate was varied systematically over a wide range covering inner scale dimensionless frequency $\omega\nu/u_\tau^2$ from 0.004 to 0.04. In terms of outer scale frequency $\omega D/u_\tau$ the corresponding values varied from 1.8 to 18. In addition, effects of changing the mean flow rate and the amplitude of flow rate pulsation were studied. Radial distributions of the amplitude of the modulation of ensemble-averaged axial velocity and the axial and radial components of RMS turbulent fluctuation, and their phase shifts relative to the imposed flow pulsation, are presented for conditions which include the *low*, *intermediate* and *high frequency* ranges. These add to and reinforce the body of information available from earlier experimental work and have enabled useful progress to be made in evaluating and validating approaches used for correlating such data. By relating observed behaviour to the fundamental processes of turbulence production, redistribution of turbulence energy between its components and radial propagation of turbulence, a good understanding of the results has been obtained.

1. Introduction

Flow in a pipe or passage where the applied pressure gradient is caused to change with time so that a periodic variation of mass flow rate is superimposed on a non-zero temporal mean value is usually referred to as pulsating flow. The condition of no-slip at the wall necessitates that in order to accommodate the imposed variation of flow rate additional vorticity must be generated in the boundary layer in a manner which varies with time. Thus coherent shear waves are excited which propagate from the wall into the fluid and are attenuated as they do so.

In the case of laminar pulsating flow, see Uchida [1], the wave attenuation is characterised by a length scale $l_s = \sqrt{2\nu/\omega}$ (in which ν is the kinematic viscosity of the fluid and ω is the radian frequency of the pulsation). This length scale is usually referred to as the Stokes layer thickness in recognition of the pioneering contribution which Stokes made to the theory of unsteady flow [2]. He showed that amplitude of the waves are attenuated by a factor e over a distance equal to l_s. Thus, the higher the frequency of the pulsation the thinner is the Stokes layer and the greater is the attenuation. This decay in shear wave amplitude is accompanied by a variation of the modulation of the local temporal mean velocity field in response to the imposed pulsation. Beyond the location where the shear wave is effectively fully-attenuated, the modulation becomes uniform and the flow can be thought of as oscillating in a 'plug flow' manner about a temporal mean distribution of velocity.

Turning next to turbulent pulsating flow, this has been of ongoing interest to researchers for over thirty five years, mainly because of its potential to provide valuable insight into some interesting fundamental aspects of the physics of turbulence. Comprehensive reviews of turbulent pulsating pipe flow studies can be found in papers by Brereton and Mankbadi [3] and Gundogdu and Carpinlioglu [4].

Taking a time mean view of a turbulent wall shear flow leads to the concept of turbulent shear stresses being present in addition to viscous stresses and enables such a flow to be considered as being steady and made up of different regions defined according to the relative magnitude of these two kinds of stress. Thus, such a flow can be thought of as consisting of a laminar sub-layer, a buffer layer and a turbulent outer layer. Turbulent pulsating flows can be viewed in a similar manner if ensemble averaging is used to process results from many experiments with nominally identical excursions of flow rate in order to decompose the velocity field into a temporal (long time) mean velocity distribution with a periodic modulation of velocity superimposed on it. Turbulent velocity fluctuations, which arise as a result of random departures of the instantaneous local velocity from the local ensemble average value,

* Corresponding author.
E-mail address: s.he@abdn.ac.uk (S. He).

0997-7546/$ – see front matter © 2008 Elsevier Masson SAS. All rights reserved.
doi:10.1016/j.euromechflu.2008.05.004

can then be calculated and phase-averaged turbulence properties determined. In this way, a turbulent pulsating flow can also be thought of in terms of regions, or layers, defined according to the relative magnitude of viscous and turbulent shear stresses.

In some very early studies of periodic unsteady turbulent flow in tubes and passages, where the imposed pulsations of flow rate were of small amplitude and at relatively high frequency, valuable progress was made, albeit by rather indirect means, in identifying appropriate scaling parameters and understanding the interactions between the propagating shear waves and the turbulence (Hussain and Reynolds [5,6], Ahrens and Ronneherger [7] Ahrens [8], Acharya and Reynolds [9] and Ronneherger [10], see Ronneberger and Ahrens [11]). At about the same time (1971) Gerrard [12] reported a pioneering experimental study of turbulent pulsating flow in which he managed to measure local instantaneous velocities in water using cine-photography. A tendency for the flow to laminarise was observed. Soon afterwards, Mizushina et al. [13,14] reported comprehensive investigations of pulsating flow in which values of phase-averaged velocity and turbulence intensity were obtained from measurements made using an electrochemical method. However, due to the experimental difficulties involved, only 20 cycles were covered. This limited the extent to which converged results could be obtained.

Further early studies of turbulent pulsating pipe flow were reported by Ramaprian and Tu [15–17] in which a single component Laser Doppler Anemometry system was used to measure local instantaneous velocity. In the first of these, attention was focused on pulsating flow at Reynolds number based on mean flow rate numbers near the transition value. This work was extended later to higher values of mean Reynolds number in the two further papers.

Several investigations of turbulent pulsating pipe flow using hot wire anemometry were reported by Shemer and co-workers. In Shemer and Wygnansky [18], attention was restricted to mean velocity only. Later, in Shemer and Kit [19], attention was focused on the time dependence of the turbulence structure in order to establish the conditions under which pulsating flow could be regarded as quasi-steady. In Shemer et al. [20] an investigation was reported in which information about the turbulent velocity components and turbulent shear stress was obtained using a rake of nine hot wires. The experiments covered a range of mean flow Reynolds number and ratio of pulsation amplitude to mean flow rate but were still restricted to relatively low frequencies. Experiments by Burnel at al. [21] supplemented the above-mentioned studies. Measurements of turbulent shear stress were made using x-type hot film probes.

In a detailed study of the response of wall shear stress in turbulent pulsating pipeflow Mao and Hanratty [22] made measurements over a wide range of frequency using an electrochemical technique. Finnicum and Hanratty [23] studied the influence of imposed flow pulsations on turbulence and Mao and Hanratty [24,25] made measurements of wall shear under conditions where the amplitude of the imposed oscillations was large. Also, an investigation of turbulent pulsating pipe flow focusing particularly on the very high frequency and high frequency ranges was reported by Hwang and Brereton [26].

Binder, Tardu and co-workers have maintained an on-going interest in turbulent pulsating flow in channels. Early studies were reported by Binder and Kueny [27] and Binder et al. [28]. Further work covering a wide range of experimental conditions was reported by Binder, Tardu and Blackwelder [29]. Velocity and wall shear stress measurements were made using a single component LDA system, focus sing mainly on the so-called logarithmic and wall regions of the boundary layer. In Tardu and Binder [30] the modulation of wall shear stress at high frequencies was studied using a flush-mounted hot-film probe. Binder, Tardu and Vezin [31] examined the cyclic modulation of turbulent stresses and length scales and Tardu and Binder [32] reported a study of the effect of flow pulsations on turbulent bursts. Recently, Tardu and da Costa [33] reported experiments in which both wall shear stress and local turbulent shear stress were measured in pulsating channel flow.

In addition to the work mentioned so far, a number of studies have been reported of the effects of imposed variation of the free stream velocity on the flow in a boundary layer on a flat plate. Examples include those of Karlsson [34], Cousteix et al. [35], Brereton et al. [36] and Brereton and Reynolds [37]. Cousteix et al. highlighted the different behaviour of the outer and inner parts of the boundary layer. Brereton et al used a two colour LDA system which enabled near-wall measurements to be made with high spatial resolution. They demonstrated that the mean structure of a turbulent boundary layer on a flat plate is sufficiently robust that the imposition of free-stream velocity variations results in only minor changes to the mean flow field. Likewise, mean levels of turbulence production were found to be relatively unaffected by free-stream velocity variation. Brereton and Reynolds focused their attention on temporal response. Interestingly, they were able to detect stages in the process of re-distribution of energy between turbulence components driven by coherent motions in the underlying mean flow close to the wall.

Relatively recently, a particularly valuable contribution to the understanding of pulsating turbulent channel flow has been made by Scotti and Poimelli [38] using Direct Numerical Simulation (DNS) and Large Eddy Simulation (LES). In comparison with physical experiments, where the number and scope of measurements are usually rather limited, their 'numerical experiments' produced detailed turbulence statistics as well as information on the topology of the coherent structures. Their results were generally consistent with experimental data reported earlier in literature and enabled them to develop a detailed picture of turbulent pulsating flow in terms of the categories based on the concept of a turbulent penetration depth suggested by Ramaprian and Tu [17]. Below, we present a summary of that picture and of the relationship between the various dimensionless scaling parameters which can be used for correlating data on turbulent pulsating flow.

If a pulsation of sufficiently high frequency is imposed on a steady turbulent flow, the shear waves propagating into the fluid from the wall will be strongly attenuated and mainly confined to the viscous sub-layer region. For this to be so, the thickness of the Stokes layer ($l_s = \sqrt{2\nu/\omega}$) must be significantly less than that of the viscous sub-layer (usually specified, as $y^+ \approx 5$, where $y^+ = yu_\tau/\nu$ in which u_τ is the friction velocity associated with the temporal mean flow). Thus $l_s^+ (= l_s u_\tau/\nu)$ should be less than about 1. Noting that the inner scale Strouhal number $\omega^+ (= \omega\nu/u_\tau^2)$ is related to l_s^+ by the expression $\omega^+ = 2/l_s^{+2}$, we see that for this condition to apply ω^+ must have a value greater than about 2.

As in the case of a completely laminar flow, the modulation of the velocity field varies across the region where the shear stress is being attenuated but becomes uniform in the region further out. Thus, for the *very high frequency* condition under consideration, the inner and outer layers are completely decoupled and the turbulence in the outer region is not affected by the imposed pulsation of flow rate. That region has the same distribution of turbulence as in a steady turbulent flow through the pipe or channel at the temporal mean mass flow rate. The velocity field in the outer region is made up of the corresponding steady state velocity field with a uniform modulation applied to it. Such a flow can be viewed as one in which the turbulence is 'frozen' and is simply being advected in a 'plug flow'. Under the conditions considered above, the response of the system to the pulsation of flow rate is at the forcing frequency and a sinusoidal response of wall shear stress is observed with the 45° phase lead seen in the laminar Stokes solution.

Some reduction of the frequency of the imposed pulsation below that for which the velocity and turbulence fields are just described, but still keeping within a *relatively high frequency* range (say, $0.2 \geqslant \omega^+ \geqslant 0.04$, for which $7 \geqslant l_s^+ \geqslant 3$), will lead to a situation where the shear waves propagate into the region beyond the viscous sub-layer where turbulent stresses are significant compared with those due to viscous action. In doing so the shear waves will interact with the steady turbulence field generated by the temporal mean flow, producing an oscillating response in the turbulence quantities. For such conditions it is helpful to make use of a concept due to Ramaprian and Tu and think in terms of a turbulent Stokes layer thickness, or turbulent penetration depth, having a thickness l_t defined using the sum of a molecular kinematic viscosity ν and a turbulent one ν_t. This provides a measure of how far shear waves generated in the wall region of a pulsating flow will penetrate into it. Following ideas presented in the paper by Scotti and Piomelli [38], if l_t is defined as $\sqrt{2(\nu+\nu_t)/\omega}$ and ν_t is represented by $\kappa u_\tau l_t$, in which κ is the Karman constant 0.4, it can be shown that $l_t = l_s[\kappa l_s^+/2 + \sqrt{(\kappa l_s^+/2)^2+1}]$. From this it can be seen that dimensionless turbulent penetration depth l_t^+ is simply a function of l_s^+. At the lowest frequency in the range under consideration now, $\omega^+ = 0.04$, l_s^+ is about 7 and l_t^+ about 22. Under such conditions, the inner and outer layers are coupled, but only very weakly. The modulation of velocity varies with distance from the wall out to a location characterised by λ_t^+ $(=2\pi l_t^+)$ and then becomes uniform. Beyond this, the flow condition is again a 'frozen' one.

Further reduction of the frequency of the pulsation into a range which might be described as being of *intermediate frequency* ($0.04 \geqslant \omega^+ \geqslant 0.01$, for which $14 \geqslant l_s^+ \geqslant 7$) leads to a stronger coupling of the inner and outer layers and a significant response of the turbulence field to the imposed pulsation. At the lowest frequency in this range, l_t^+ is about 80. For such conditions, phase-averaged quantities such as turbulent kinetic energy no longer vary with time in a sinusoidal manner. The velocity c with which the shear waves propagate into the flow is given by λ_t/T, where λ_t $(=2\pi l_t)$ is the wave length and T $(=2\pi/\omega)$ is the time period of the oscillation. It follows that $c = \omega l_t$ and so, noting that for $\kappa l_s^+/2 \gg 1$ the dimensionless turbulent penetration depth l_t^+ tends to $\kappa {l_s^+}^2$, we find that $c = 2\kappa u_\tau$. Thus, the velocity of the shear wave only depends on the friction velocity and, since the Karman constant κ has the value 0.4, the wave propagation velocity is $0.8u_\tau$, that is, almost equal to u_τ. This compares favourably with $u_\tau/\sqrt{2}$ obtained by the present authors from experiments on an accelerating pipe flow [39].

Beyond the edge of the turbulent penetration region the velocity modulation is again uniform and the turbulence field is in a 'frozen' condition. The magnitude of the wavelength λ_t in relation to the pipe radius R, is a dimensionless parameter which characterises the extent to which pulsating flows in this frequency range are frozen in the outer region. It is of interest to note that λ_t/R is inversely proportional to the outer scale Strouhal number or scaling parameter $\omega D/u_\tau$, in which D is the pipe diameter.

The extent of the 'frozen' region diminishes systematically as the frequency of the flow pulsation is reduced until eventually $\lambda_t = R$ and there is no such region. The outer scaling parameter for frequency $\omega D/u_\tau$ then has a value of about 10. The time for a shear wave to travel across the flow from the near-wall region to the centre, which is given by the ratio of the pipe radius to the wave velocity, is then equal to the time period T of the imposed oscillation. For convenience, an alternative outer scaling parameter T^* $(= Tu_\tau/R \approx \lambda_t/R)$ can be defined which will have a value of about unity when the shear waves propagate right to the centre of the pipe or channel. It is inversely proportional to the outer scaling parameter for frequency $\omega D/u_\tau$. For conditions where T^* is greater than unity the entire flow will be affected by the imposed unsteadiness. In this *low frequency* range, moving across the flow, production and dissipation of turbulence become out of phase with respect to each other and the acceleration and deceleration stages of the pulsation cycle exhibit significant asymmetry which varies with radial position.

If the frequency of the imposed pulsation is reduced to a value such that the time for a shear wave to travel across the flow from the near wall region to the centre is very small compared with the time period of the imposed oscillation, the turbulence will have time to relax to local (in time) equilibrium. The phases of each of the turbulence quantities then become independent of position and the velocity and turbulence distributions will be similar to those of a steady flow through the pipe or channel at a flow rate equal to the instantaneous value. Such a pulsating flow can be described as being *quasi-steady*. The criterion for this condition to be achieved, is $Tu_\tau/R \gg 1$,which can be re-expressed as $\omega D/u_\tau \ll 10$.

In summary, the non-dimensional parameters that have been proposed for use in pulsating turbulent pipe flow basically have two different forms. The Stokes–Reynolds number l_s^+ $(= u_\tau\sqrt{2/(\omega\nu)})$, and the related parameter ω^+ $(=\omega\nu/u_\tau^2)$, are both associated with inner scaling. The Strouhal number $\omega D/u_\tau$, and the related parameter T^* $(= u_\tau T/R)$, are both associated with outer scaling.

The foregoing review has shown that there has been an ongoing interest of pulsating flow in pipes, channels and boundary layers and that large amounts of experimental data have been collected for each of these flow configurations. Nevertheless there is clearly still considerable scope for reinforcing the data base by further experimental study. The work described in the present paper is aimed at contributing to the body of knowledge on pulsating flow in a *pipe*, especially focusing on interactions, in the core region, between the imposed flow unsteadiness and the ensemble averaged mean flow and turbulent fields. Information on the radial as well as the axial velocity components was obtained using a two-component laser Doppler anemometer. Previous studies which fall into this category have only covered a rather limited range of flow conditions, especially in terms of frequency. The most widely cited studies of this kind are those of Tu and Ramaprian [16] and Shemer and co-workers [20]. Tu and Ramaprian conducted detailed measurements using a single component laser Doppler anemometer system but only at two frequencies (one of which was relatively high and the other quite low) and Shemer and co-workers focused exclusively on quite low frequencies. Very few two-component flow measurements have been made in pulsating pipeflow. In the experimental work reported in the present paper, the frequency was varied systematically to cover relatively high, intermediate and low frequency cases with l_s^+ in the range, $7 < l_s^+ < 23$. Under such conditions, the response of velocity and turbulence to the imposed flow unsteadiness in the core region of the flow exhibit some particularly interesting characteristics. Very high frequency and very low frequency quasi-steady, flows were not covered in this study. However the effects of varying the mean flow and the amplitude of the flow pulsation were covered.

In addition to making direct comparisons between our data and those of Tu and Ramaprian [16] and Shemer and co-workers [20], results obtained in investigations of pulsating channel and boundary flows are also discussed in relation to those obtained in the present study. Of particular relevance are the extensive studies over many years of pulsating channels of Binder, Tardu and co-workers [27–33]. Their main focus has largely been in the near-wall region. Studies were conducted with careful conditioning of the flow at the entrance and measurements were taken at a location thirteen hydraulic diameters (2 × channel height) downstream of the flow entrance. Results due to Brereton, Reynolds and co-workers [26,36,37], which were conducted for pulsating bound-

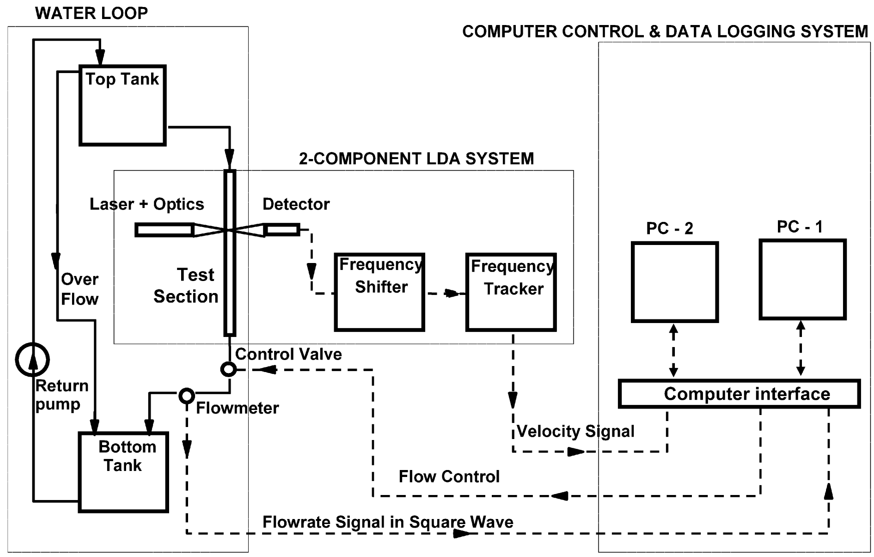

Fig. 1. Experimental facility, instrumentation and measurement systems.

ary layer flows, are also considered in relation to those from the present study. The *near-wall behaviour* investigated in the above-mentioned studies are directly relevant to the present studies. In addition, the computational study by Scotti and Piomelli [38] of pulsating channel flow has provided valuable detailed information which is difficult to obtain experimentally. Direct comparisons with such data are made wherever possible although the differences between those studies and the present one should be borne in mind. In addition to the difference in flow passage geometry, the method by which the variation of the flow was achieved was also different in the computational study. It was caused by specifying a variation of pressure, whereas in the present study and the previous experimental ones, variations of mass flow rate were imposed.

2. Analysis

Due to the periodic nature of pulsating turbulent flow, the instantaneous velocity $g(y,t)$, which is made up of the three components, u, v and w, can be decomposed into three parts:

$$g(y,t) = \bar{g}(y) + \tilde{g}(y,\phi) + g''(y,t) \tag{1}$$

in which $\bar{g}(y)$ is the (long) time mean velocity, $\tilde{g}(y,\phi)$ the periodic component (velocity *modulation*), and $g''(y,t)$ the turbulent fluctuation. The sum $\bar{g}(y) + \tilde{g}(y,\phi)$ is the ensemble-averaged velocity, $\langle g(y,\phi)\rangle$. Thus,

$$g(y,t) = \langle g(y,\phi)\rangle + g''(y,t) \tag{2}$$

The ensemble-averaged root-mean-square (rms) of the components of the turbulent fluctuations φ' (where φ' is u', v' or w') is defined by:

$$\varphi' = \left(\langle \varphi''^2\rangle\right)^{1/2} = \left[\left\langle\left(\varphi - \langle\varphi\rangle\right)^2\right\rangle\right]^{1/2} \tag{3}$$

and the ensemble averaged 'Reynolds shear stress' $-\langle uv\rangle$ is defined as:

$$-\langle uv\rangle = -\left\langle\left(u - \langle u\rangle\right)\left(v - \langle v\rangle\right)\right\rangle \tag{4}$$

The ensemble-averaged turbulence quantities (u', v', w' and $\langle uv\rangle$) can also be decomposed into components: a long time mean component and a periodic one; the latter will be called the *modulation* of the ensemble-averaged turbulence quantities.

Assuming that the flow is not only periodic, but also harmonic, the periodic component $g(y,\phi)$ may then be represented by the real part of the exponential

$$\langle g(y,\phi)\rangle = \mathrm{Real}\left\{\left[\langle g(y)\rangle\right]\exp\left(i\left(\omega t - \phi_g(y)\right)\right)\right\} \tag{5}$$

where $[\langle g(y)\rangle]$ is the amplitude of the pulsation (or modulation) and $\phi_g(y)$ is a phase lag angle. When the flow is periodic but not strictly harmonic, the time-dependent variable can be expanded in Fourier series, and the right-hand side of the above equation will represent the leading term in the expansion. It can be seen that the variables describing a fully developed pulsating pipe flow are the amplitude and frequency of the imposed unsteadiness and the mean flow rate. Although in the present study the imposed flow pulsation was sinusoidal, the ensemble averaged mean velocity and turbulence quantities were not exactly harmonic. Therefore in the data processing stage, we used the Fourier analysis technique to decompose the ensemble averaged mean velocity and turbulence quantities. Our study is mainly based on analysing the amplitude and phase angle of the leading terms of the variables.

3. Experimental details

The experimental facility and measurement equipment used in this investigation is shown in Fig. 1. It was initially designed for a study of ramp type transient flow, He and Jackson [39]. A detailed description of the facility can be found in that paper along with information on validation and calibration. Here, we have tried to provide sufficient in the way of information whilst avoiding going into too much detail.

The experiments were carried out with water flowing in a circular pipe of internal diameter 50.8 mm. A very long test section, of length to diameter ratio 130, was used to ensure that a fully developed flow was achieved in it. Flow control was achieved using computer PC-1 in conjunction with an electronic position controller and a pneumatic activator. A prescribed flow rate was converted to a valve-opening signal by the computer and sent to the electronic position controller. The latter then drove the pneumatic activator to operate the valve until the demanded opening had been achieved. Very accurate flow control with really excellent repeatability was achieved. The flow rate was measured by a turbine flow meter, the electronic output signal from which was of square-wave form with a frequency proportional to flow rate. The frequency of the signal was determined using the computer by measuring the time interval of the square wave using a standard-clock module.

A two-component laser Doppler anemometer system linked to computer PC-2 was used to make simultaneous measurements

Table 1
Experimental plan

Experiment	Mean Re	Amp %	T (s)	l_s^+	l_t^+	$\omega^+ = \frac{\omega\nu}{u_\tau^2}$	$\frac{\omega D}{u_\tau}$	$T^* = \frac{Tu_\tau}{R}$
T2(T2RE7A20)*	7000	20	2	7.2	23	0.0388	17.73	0.56
T3(T3RE7A20)	7000	20	3	8.8	33	0.0259	11.82	0.85
T4(T4RE7A20)	7000	20	4	10.2	44	0.0194	8.87	1.13
T6(T6RE7A20)	7000	20	6	12.4	64	0.0129	5.91	1.70
T10(T10RE7A20)	7000	20	10	16.1	106	0.0078	3.55	2.80
T20(T20RE7A20)	7000	20	20	22.7	209	0.0039	1.78	5.6
T3RE10A20	10 500	20	3	12.5	65	0.0128	8.31	1.21
T4.2RE10A20	10 500	20	4.22	14.8	90	0.0091	5.91	1.70
T3.3RE14A20	14 000	20	3.26	17.3	122	0.0067	5.76	1.74
T4.2RE10.5A47	10 500	47	4.22	14.8	90	0.0091	5.91	1.70

* Note: Short names, such as T2, T3, rather than the full identifiers (T2RE7A20, T3RE7A20) are used in the text whenever no confusion is expected.

of the axial and radial components of the instantaneous velocity field. In order to facilitate the measurement of turbulent velocity fluctuations of small amplitude and to improve the quality of the LDA signal, a Bragg cell and a beam expander were added to the basic optical configuration. A rectangular box made of glass sheets filled with water surrounded the glass tubing to reduce the effect of the refraction of the light due to the curvature of the tube. The dimensions of the LDA measuring volume were 0.053 mm × 0.053 mm × 0.71 mm or 0.5 × 0.5 × 7 in wall units based on the typical mean flow rate ($Re = 7000$). The nearest point of measurement from the wall, was about 12 wall units i.e., $y^+ = 12$, where $y^+ = yu_\tau/\nu$, in which u_τ is the friction velocity. The sample rate was typically 4 kHz. Data reduction was based on ensemble averaging the results from numerous successive flow pulsations. In preliminary experiments performed in our earlier study, it was found that very many samples (in excess of a thousand) were needed to enable converged values of local ensemble-averaged mean velocity and root mean square velocity to be obtained. An approach, which involved dividing the period of a transient into a number of windows and applying the conventional ensemble average procedure to the windows rather than to single points, was developed. Typically, 160 'windows' were used over a cycle. This number was determined by experimentation, minimising the scatter of processed data but at the same time ensuring that the effect on the values of the ensemble averaged quantities obtained was negligible [39]. This method reduced the number of repeated experiments needed to a few hundred. For the majority of the results presented here, 300 cycles were used in each experiment.

In the majority of the experiments, the Reynolds number based on the time mean value of the flow rate was 7000 and the amplitude (peak to mean) was 20% of the mean value. The time period of the pulsation was varied systematically from 2 to 20 seconds covering a range of non-dimensional frequency parameter ω^+ $(= \omega\nu/u_\tau^2)$ from 0.04 to 0.004. The value of the friction velocity u_τ $(= \sqrt{\tau_w/\rho})$ referred to here, and used later in the paper for calculating non-dimensional parameters was calculated using the Blasius equation $f = 0.079Re^{-1/4}$, where $f = \tau_w/(\rho U^2/2)$. The Reynolds number is based on measured mass flow rate of the mean flow, unless stated otherwise. Experiments with higher values of mean Reynolds number (10 500 and 14 000) and a higher value of the ratio of flow rate amplitude to mean value (47%) were also conducted. The experimental conditions together with values of various non-dimensional parameters are shown in Table 1.

4. Presentation of experimental results

In this paper, the amplitudes of the modulation of mean velocity and turbulence quantities are presented in a normalised form as described below. Sectionally averaged amplitudes for corresponding steady flow conditions have been used for the normalisation. These were obtained from measurements made in a series of steady state experiments at various flow rates. The averaged amplitude used for ensemble averaged mean velocity $\langle U\rangle$ can be expressed as:

$$U_N = \frac{1}{\pi R^2}\int_0^R 2\pi r\big[\langle U(r)\rangle\big]_{\text{pseudosteady}}\,dr = \frac{2}{R^2}\int_0^R r\big[\langle U(r)\rangle\big]_{\text{pseudosteady}}\,dr \qquad (6)$$

Similarly, for the ensemble averaged rms velocities u' and v',

$$u'_N = \frac{2}{R^2}\int_0^R r\big[u'(r)\big]_{\text{pseudosteady}}\,dr \qquad (7)$$

$$v'_N = \frac{2}{R^2}\int_0^R r\big[v'(r)\big]_{\text{pseudosteady}}\,dr \qquad (8)$$

If the Reynolds number of the mean flow and the amplitude of the flow pulsation are kept constant, the sectionally averaged amplitude of the velocity modulation will be the same for pulsations of different frequencies. However, when the Reynolds number of the mean flow or the amplitude of the flow pulsation are varied, the sectionally averaged amplitude varies. Therefore, in order to be able to compare the results easily for all the cases covered in the present study, it was helpful to normalise the amplitude using values of U_N as defined above. This brought all the radial distributions of the amplitude of velocity modulation for different transients to approximately the same mean level, i.e., around unity. The detailed shapes of the distributions could then be readily compared with each other to examine the effect on the amplitude of velocity modulation of the imposed flow pulsation.

As far as the turbulence quantities are concerned, the flow pulsation not only affects the shape of the radial distribution of the modulation but also the sectionally averaged amplitude. This is because the flow pulsation can affect the level of the response of turbulence quantities. In this case, the normalisation of the modulation of turbulence quantities enables the results from experiments with flow pulsations of different amplitude, frequency and mean Reynolds number to be readily compared both in terms of shape and the mean level relative to that for the quasi-steady condition. This provides an indication of how much the response of turbulence is attenuated in a transient and where this attenuation occurs.

5. Discussion of results

5.1. Ensemble averaged velocity field – amplitude of velocity modulation

Fig. 2(a) shows radial distributions of normalised amplitude of velocity modulation obtained in experiments with imposed pulsations of flow rate covering a range of time periods from 20 seconds down to 2 seconds with a fixed value of mean Reynolds number of 7000 and a ratio of pulsation amplitude to mean flow rate of 0.2. They exhibit a non-monotonic pattern of behaviour with increase of pulsation frequency. Considering first the lowest frequency case, experiment T20, it can be seen that the distribution is quite similar to that produced using the steady state measurements. The amplitude is highest at the centre of the pipe and diminishes with distance from it. With increase of frequency, reduction of the time period, the flow in the central region fails to respond fully to the imposed pulsation with the result that the amplitude of velocity modulation there is reduced. Accordingly, the peak on the distribution shifts away from the centre. The higher the frequency, the

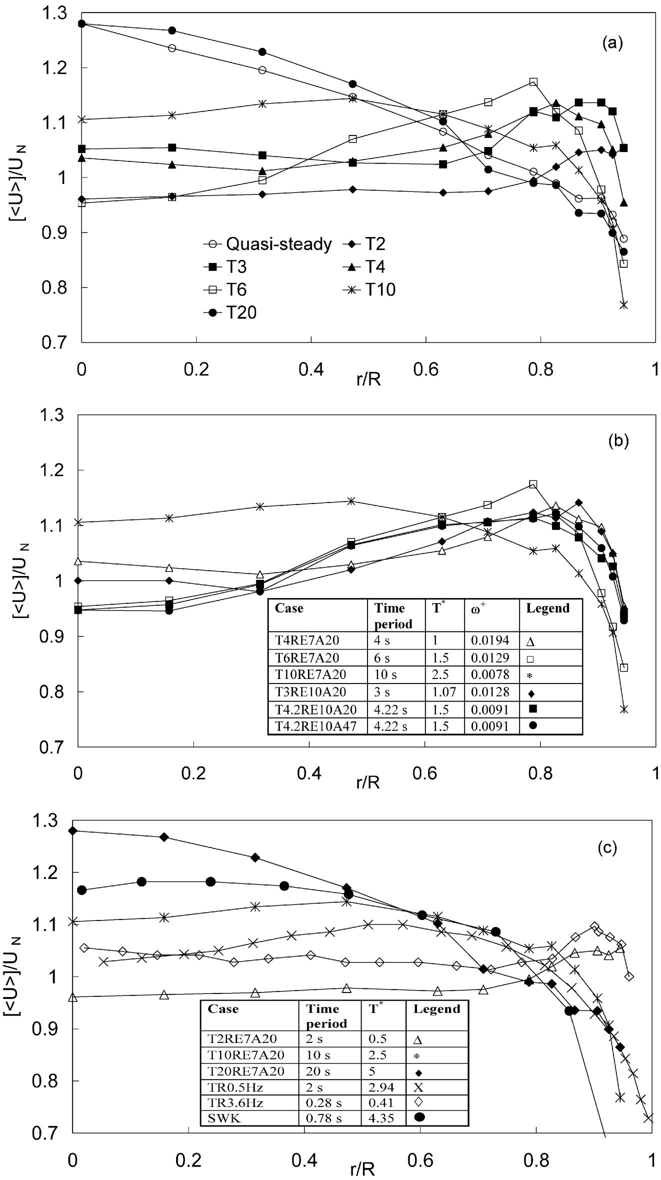

Case	Time period	T^*	ω^+	Legend
T4RE7A20	4 s	1	0.0194	Δ
T6RE7A20	6 s	1.5	0.0129	□
T10RE7A20	10 s	2.5	0.0078	*
T3RE10A20	3 s	1.07	0.0128	♦
T4.2RE10A20	4.22 s	1.5	0.0091	■
T4.2RE10A47	4.22 s	1.5	0.0091	●

Case	Time period	T^*	Legend
T2RE7A20	2 s	0.5	Δ
T10RE7A20	10 s	2.5	*
T20RE7A20	20 s	5	♦
TR0.5Hz	2 s	2.94	X
TR3.6Hz	0.28 s	0.41	◇
SWK	0.78 s	4.35	●

Fig. 2. Amplitude of velocity modulation in pulsating flows, (a) effect of varying time periods, (b) effect of varying the mean flow rate and amplitude of the pulsation, (c) comparison with results from Ramaprian and Tu (TR) [16] and Shemer et al. (SWK) [20].

further away the peak is from the centre. For the mid-frequency case, T6, the amplitude of velocity modulation at the centre of the pipe becomes less than the mean. As will be seen later the response of turbulence in the central region for this condition lags behind the imposed pulsation of the flow by more than 180°. When the frequency of the pulsation is increased further (experiments T4, T3, T2), the flow in the central part of the pipe becomes 'frozen'. The extent of the 'frozen' region increases as the frequency of the pulsation increases. For the highest frequency case, experiment T2, the flow is effectively 'frozen' over much of the radius. It pulsates with uniform modulation in a plug flow manner. Under these conditions, the inner and outer layers are, effectively, decoupled and the influence of the imposed pulsation of flow rate on the amplitude of the modulation of velocity is restricted to the inner layer only.

Fig. 2(b) shows the effects on the amplitude of velocity modulation of varying the mean Reynolds number and the ratio of the pulsation amplitude to the mean flow rate. It is clear that the results of experiments with the same pulsation period but different

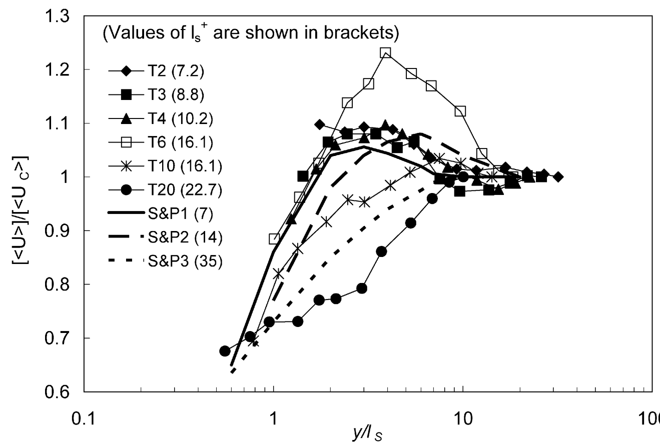

Fig. 3. Normalised amplitude of velocity modulation plotted against y/l_s, comparison with data from Scotti and Piomelli [38].

values of mean flow rate exhibit different characteristics. However, comparisons need to be made on an appropriate non-dimensional basis. Values of two different non-dimensional parameters, the outer scaling parameter T^* and the inner scaling parameter ω^+, are shown together within the legend on the figure. It can be seen that the overall variation of amplitude of velocity modulation in the outer region is quite similar for cases where the values of the outer scaling parameter T^* are the same (Case T4RE7A20 cf. T3RE10A20; and Case T6RE7A20 cf. T4.2RE10A20), whereas, when the inner parameter ω^+ is the same, the data do not correlate (Case T6RE7A20 cf. Case T3RE10A20). The inner scaling parameter, although appropriate for characterising the near wall flow, is not suitable when the overall behaviour is considered. It can also be seen from Fig. 2(b) that the amplitude of the flow pulsation has no significant effect (compare Case T4.2RE10A20 with T4.2RE10A47). This observation is consistent with what has been found in earlier studies.

Measurements of the radial distribution of amplitude of velocity modulation have been reported by Tu and Ramaprian [16] and also by Shemer and co-workers [20]. Tu and Ramaprian studied two cases, a low frequency one for which $T^* = 3.24$ (Case TR0.5Hz) and a relatively high frequency one for which $T^* = 0.45$ (Case TR3.6Hz). As can be seen from Fig. 2(c), the radial distribution of amplitude of velocity modulation for the lower frequency case, TR0.5Hz, is very similar to that of experiment T10 in the present study which has a similar value of T^* (2.8). For the higher frequency case (Case TR3.6Hz), the radial distribution is similar to that in our experiment T2, for which $T^* = 0.56$. In this case the radial distribution is flat over most of the core region and the peak is achieved at a location very close to the wall. Clearly, these two rather unconnected results from the study of Tu and Ramaprian fit nicely into the expected picture relating amplitude of velocity modulation to pulsation frequency. Furthermore, the parameter T^* correlates the data quite well.

Shemer et al. focused on pulsations of relatively low frequency. A typical result from that source is shown in Fig. 2(c) and referred to there as SWK. For that experiment the parameter T^* had the value 4.78. Comparing the shape of the SWK distribution with those for experiments T10 and T20 of the present study (for which $T^* = 2.8$ and 5.6 respectively) some consistency can be seen. The peak has just moved away from the centre but not as far as in T10, which has a lower value of T^*.

In Fig. 3, comparisons of amplitude of velocity modulation obtained in the present investigation, normalises using the value at the centre, are made with values from the LES study of pulsating channel flow reported by Scotti and Piomelli [38]. These are plotted against y/l_s using logarithmic scales, because the focus is on the near-wall region (direct comparison in the core is less appropriate considering the difference in flow passage geometry, a plane channel and a pipe). When presented in this manner the results from our experiments at higher frequencies (T2, T3 and T4) and those from the higher frequency case S&P1 of the LES study, exhibit a tendency to correlate in the wall region. Also, the results for the lower frequencies (T10 and T20) from the present study show a trend similar to the slow pulsating flow case from the LES study (S&P3). The results of Tardu et al. [29] show a very similar trend as well, (see the comparison made in Scotti and Piomelli [38]). Experiment T6 of the present study is of special interest because the amplitude of velocity modulation in the region between the wall and the core is much higher than in all the other cases. This is indicative of a particularly strong interaction between imposed flow pulsation and turbulence, occurring at an intermediate frequency. Interestingly, for such a condition, the mean velocity at the centre of the pipe reaches a minimum (see Fig. 2(a)).

5.2. Phase shift of the modulation of local mean velocity

Fig. 4(a) shows the radial distributions of the phase shift of ensemble averaged velocity relative to the imposed pulsation of the flow rate for experiments T2 to T20. It can be seen that in the higher frequency range (experiments T2, T3, T4), the phase shift in the core region is close to zero. In that region of 'frozen' flow the fluid moves in phase with the imposed pulsation. The extent of the region where the phase shift is zero reduces with decrease of frequency until eventually there is no such region. With further reduction of frequency, experiments T6 and T10, delays build up in the central region. Thus for flows with such 'mid-range' frequencies, a relatively large positive phase shift develops between the response of velocity near the wall and that in the core region. However, when the pulsation frequency is reduced even further, case T20, the delay in the central region starts to reduce and the distribution of phase shift becomes more uniform.

The behaviour is very different in the wall region. Two distinct patterns can be identified. For the higher frequency cases, the velocity near the wall responds faster than the mean flow, i.e. there is a phase advance in that region and the phase shift is negative. The nearer the wall, the greater is the phase advance. With reduction of frequency, after an initial increase, the phase advance (or negative phase shift) starts to reduce as the wall is approached, until eventually the velocity lags behind the mean flow again. An increase of the phase shift of velocity as the wall is approached has also been reported by Tu and Ramaprian [16] and Shemer et al. [20]. Those authors described this as a 'surprising' feature and attributed it to a relatively slow adaptation of turbulence to the local flow conditions.

The phase shift of velocity relative to the imposed flow pulsation in the experiments with different values of mean Reynolds number is shown in Fig. 4(b). Also shown in this figure are the results from the experiment with a larger ratio of amplitude to mean flow rate. As was the case with the distributions of amplitude of velocity modulation, the outer scale parameter T^* again appears to correlate the data for different values of mean flow Reynolds number fairly well. Also, it can be seen that again there is not a noticeable effect of changing the amplitude to mean ratio.

Fig. 4(c) shows comparisons between the phase shifts of velocity modulation found in the present study and in the studies of Tu and Ramaprian [16] and Shemer et al. [20]. It can be seen from the figure that the Tu and Ramaprian results compare favourably with those from the present study on the basis of the outer scaling parameter T^*. The higher frequency case reported in Tu and Ramaprian, TR3.6 Hz, clearly shows a near-to-zero phase shift in the core and a phase advance near the wall. The distribution is very close to that for case T2 of the present study which has a similar value of T^*. The lower frequency case TR0.5 Hz, exhibits a large delay in the centre as in case T10 of the present study. The phase shift data of Shemer et al. was related to an imposed pressure pulsation rather than a measured pulsation of flow rate. A flow to pressure phase shift (constant across the radius) has been assumed in order to move the Shemer et al profile down to a level directly comparable to that of the present results. Since our main concern here is with the shape of the distribution, the fact that there are some uncertainties involved due to the above-mentioned adjustment should not invalidate the comparison. Shemer et al.'s. experimental data show a small delay in the centre of the pipe but an increased one in the region near the wall. This can be compared directly with that of our experiment T20, for which T^* was similar. The observed trends are similar.

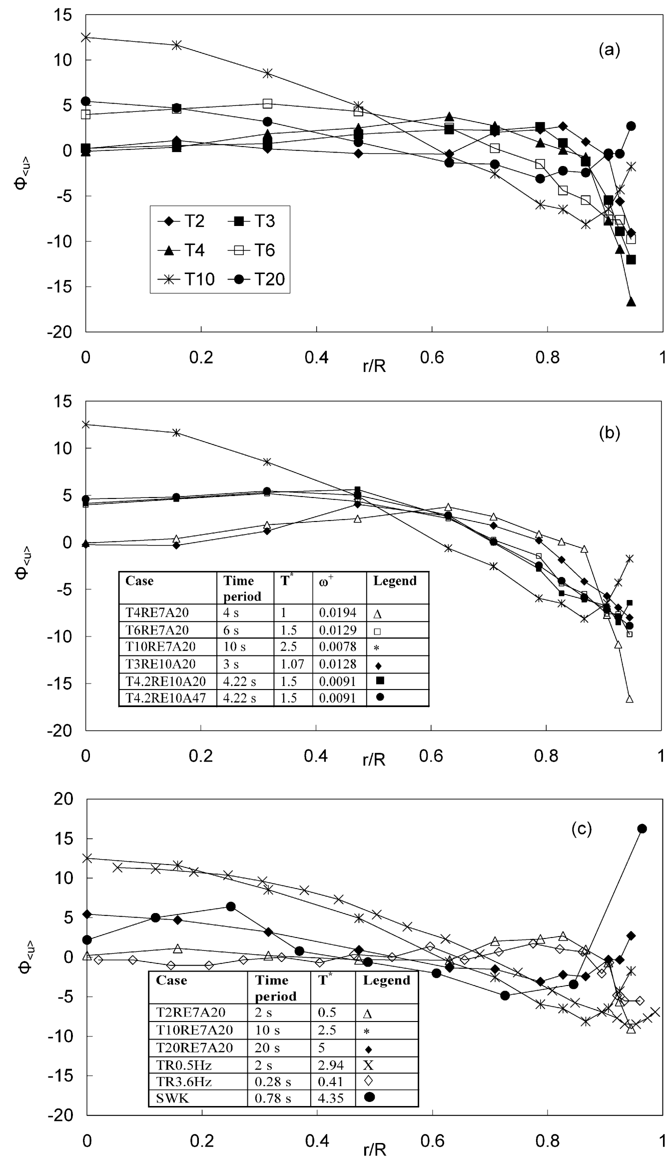

Fig. 4. Phase shift of velocity modulation relative to the imposed flow pulsation. (a) effect of varying the time period of the pulsation, (b) effect of varying the mean flow and amplitude of the flow pulsation, (c) comparison with results of Ramaprian and Tu (TR) and Shemer et al. (SWK).

5.3. Amplitude of the modulation of turbulence quantities

Fig. 5 shows the distributions of normalised amplitude of the modulation of the radial and axial components of rms turbulent fluctuations from experiments T2 to T20. It can be seen that when

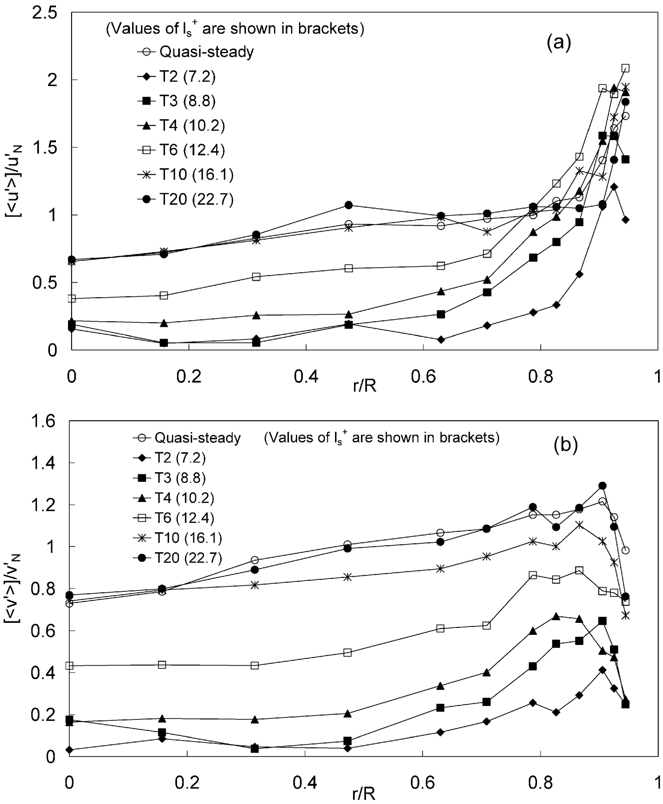

Fig. 5. Amplitude of the modulation of rms turbulent fluctuations – effect of varying the time period of the imposed flow pulsation with constant mean flow and amplitude. (a) axial component (u'), (b) radial component (v').

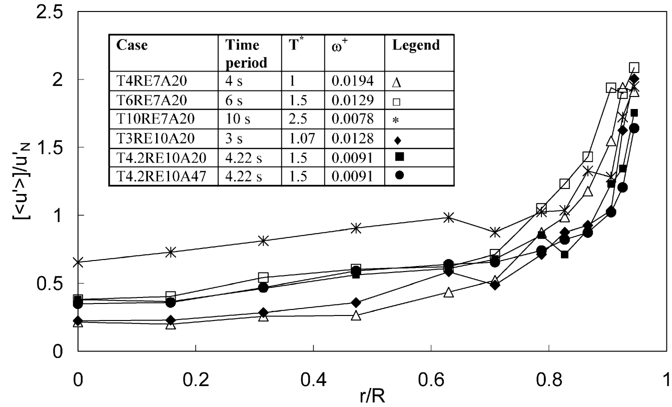

Fig. 6. Amplitude of the modulation of rms fluctuation of axial velocity u' – effect of varying the mean flow rate and amplitude of the flow rate pulsation.

the frequency of the imposed transient is low, as in case T20, the modulation of u' and v' are both in close agreement with the distributions produced using the steady flow measurements. With increase in the frequency of the imposed pulsation, the amplitude of the modulation reduces in the core region. In the two highest frequency cases, T3 and T2, the amplitudes are close to zero in that region, and the turbulence quantities are effectively 'frozen'. This is entirely consistent with the behaviour seen earlier in the results for ensemble averaged axial mean velocity. Thus, for such conditions the entire flow structure in the core region, both mean flow and turbulence, is 'frozen'.

Next, focusing on the near-wall region, it can be seen that the responses of u' and v' are very different. The variation with frequency of the amplitude of the u' modulation is non-monotonic. Firstly, as the frequency is increased (experiments T20 through to T6), the amplitude of the u' modulation increases slightly. It then starts to reduce as the frequency is increased further (experiments T4 through to T2). In contrast, the amplitude of the v' modulation falls systematically with increase of frequency for experiments T20 through to T2 as it did in the core. The difference between the behaviour of u' and v' has to be considered in the context of two different phenomena, the decoupling of the wall layer and the core flow, which develops under conditions of high frequency, and the process of energy transfer between the u and v components which takes place in the near-wall region. These matters will be discussed in more detail in Section 6.

The distributions of the amplitude of modulation of u' in the experiments with different mean Reynolds numbers, and also in the case with a larger ratio of pulsation amplitude to mean flow rate, are shown in Fig. 6. In the core region the non-dimensional outer scale parameter T^* again seems to correlate the data. However, as expected it fails to do so near the wall. Also, from Fig. 6 it can be seen that variation of the amplitude of the flow pulsation has little effect on the response of turbulence (compare T4.2RE10A20 with T4.2RE10A47). Similar conclusions concerning the influences of time mean Reynolds number and amplitude to mean flow rate were arrived at in the case of the v' data produced in this study (not presented here).

Direct comparisons of data on the amplitude of the modulation of turbulence quantities from different experimental studies are difficult to make as the parameters required for normalisations which are needed to bring together data are not always readily available. However the general trends can be compared. For pipe flows, values of u' obtained using a single component LDA system were reported in Tu and Ramaprian [16] for their two cases, TR0.5 Hz and TR3.6 Hz. In the latter ($T^* = 0.45$), u' was frozen over a large part of the core region. In the other case ($T^* = 3.24$), the amplitude of the modulation of u' was found to be similar to that for quasi-steady flow. These features are consistent with the general picture seen in the present study. As indicated earlier, the experiments of Shemer et al. [20] were limited to quite low frequencies. Thus, the amplitudes of the modulation of the turbulence fluctuations in their experiments deviated only marginally from the corresponding quasi-steady values. The near-wall behaviour of amplitude of the modulation of turbulence in pulsating channel flow was obtained for values of l_s^+ from about 34 down to about 4 by Scotti and Piomelli [38] and Tardu et al. [29]. The amplitude reduced systematically with decreasing l_s^+. This is in contrast with the finding in the present study that the peak amplitude of u' only starts to reduce for $l_s^+ < 10$ (Fig. 5(a)). We do not have an explanation of this difference in behaviour.

5.4. Delays in the response of turbulence relative to the imposed flow pulsation

Fig. 7 shows the radial distributions of the phase shifts of the modulation of u' and v' relative to the imposed flow pulsation for experiments T2 to T20. No phase shift information is available in the central region of the pipe for the higher frequency cases because, as was seen earlier in Fig. 5, the turbulence there is frozen. The general behaviour of the distributions of phase shift is rather similar in the case of each of the two turbulence components. The shift is smallest for the lowest frequency experiment and it increases monotonically with the increase of frequency. In each case, the phase shift is smallest in the region near the wall and increases with distance from it. The rate of increase with distance from the wall is relatively small in the case of the lower frequency flow rate pulsations but becomes systematically bigger with increase of frequency.

Alternatively, the response of turbulence can be described in terms of absolute time delay relative to the imposed flow pulsa-

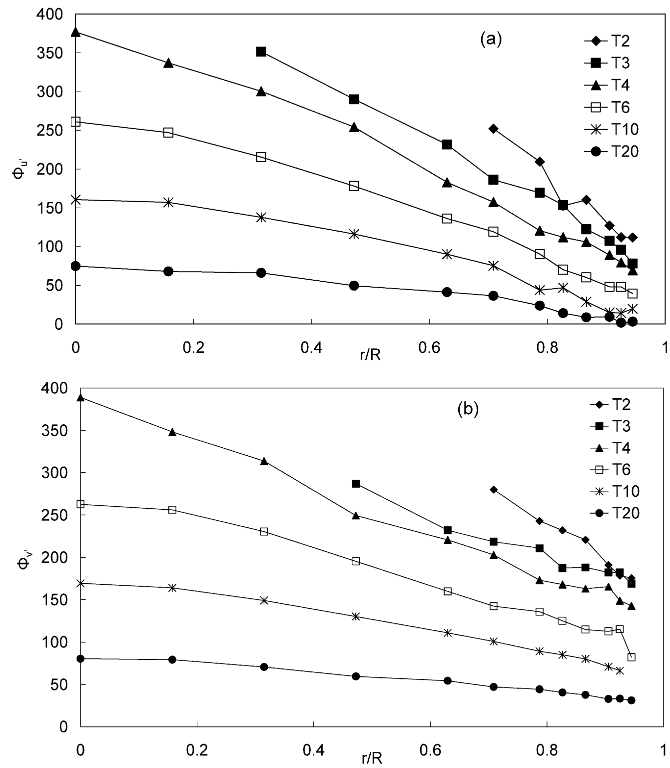

Fig. 7. Phase shift relative to the imposed flow pulsation of the modulation of rms fluctuation. (a) axial component (u'), (b) radial component (v').

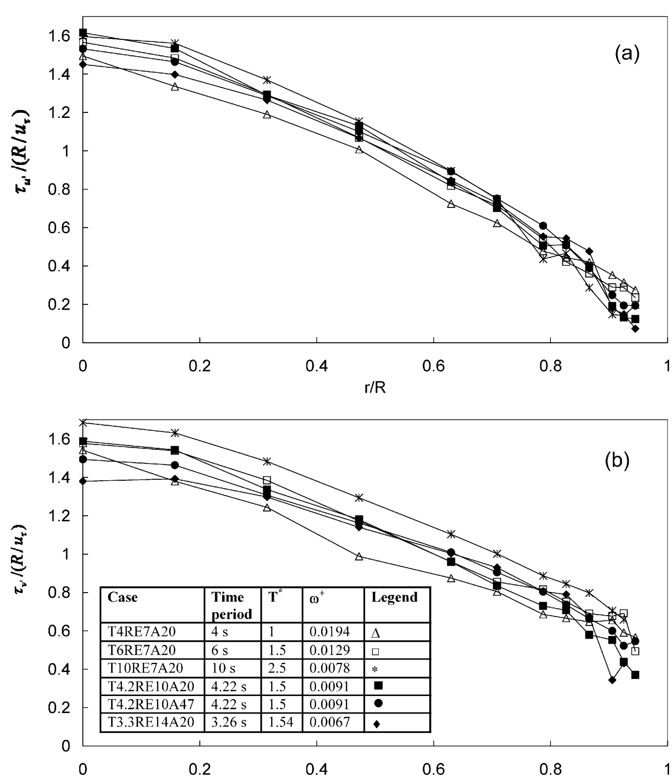

Fig. 8. Normalises time delay relative to the imposed flow pulsation of the modulation of rms fluctuation. (a) axial component (u'), (b) radial component (v').

tion. Such delays normalised using R/u_τ are shown in Fig. 8 for cases with different values of mean Reynolds number, pulsation amplitude and time period. The delays for the various cases are

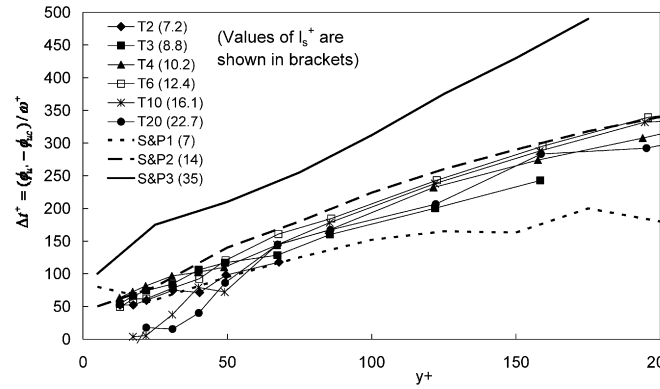

Fig. 9. Comparison of time delay (relative to velocity at the centre) of the modulation of axial component of rms fluctuation with data of Scotti and Piomelli [38].

fairly well correlated irrespective of the wide range of conditions considered. The minimum delay at the measuring point nearest to the wall is clearly different for u' and v': It is very small in the case of u' but much greater in the case of v'. In the core region, the behaviour of the delays in u' and v' are rather similar. The slope of the curves for both u' and v' remain fairly constant over almost the entire core region of the flow, which indicates that the speed of radial propagation of turbulence is approximately constant. A closer inspection of the data indicates a small yet systematic reduction in the delay as the pulsation frequency increases, but the slope of the curves remains more or less the same. That is, the speed of the propagation is not affected by the frequency of the pulsation of the flow.

Fig. 9 shows comparisons of the time delay relative to the velocity at the centre of the modulation of the axial component of rms turbulent fluctuation with data from Scotti and Piomelli [38]. The delay is normalised using ω^+ and plotted against y^+ because the comparison is mainly applicable in the wall region. The agreement between the results from the two studies is excellent for the higher to medium frequency cases. When the pulsation frequency is very low ($l_s^+ = 35$), the data of Scotti and Piomelli indicate that the delay increases significantly. The slowest case of the present study ($l_s^+ = 22.7$) does not, however, show such tendency. The most striking difference is the response in near-wall region where the LES result indicates a significant delay for the lowest frequency case but the results from the present study show almost no delay for the two lower frequency flows. Clearly, there are some differences between the two studies that might be responsible for the different behaviour. Firstly, as explained earlier, a pulsating pressure gradient was used to generate the unsteady flow in the LES simulations, whereas a pulsating mass flow was imposed in the present experiments. In addition, the delays are presented relative to the response of the velocity at the centre of the flow which might be rather different in pipeflow and channel flow.

6. Further discussion

As mentioned earlier, the present authors have reported a detailed investigation of the response of turbulence during ramp-type excursions of flow rate in a pipe [39]. It was found that the observed response of turbulence to such flow transients could be related to the processes of turbulence production in the wall region, redistribution of turbulent kinetic energy between components and diffusion of turbulence into and across the core. Delays associated with the finite time scales involved in each of these processes played an important part in the overall response of the flow to the imposed excursions of flow rate. After the initiation of a flow excursion, turbulence first began to respond in the near-wall region after a short delay associated with production. Initially, a response was only observed in the axial component u'. Then, after a further delay, the v' and w' components started to respond, gaining energy from the u' component. The near-wall response then propagated progressively towards the centre of the pipe at a speed which was found to be proportional to $u_{\tau 0}$, the friction velocity based on the value of flow rate at the start of the excursion.

In the pulsating flows under consideration here, the variation of flow rate with time is harmonic rather than linear. However, one might expect that the essential physical processes involved in these two types of flow would be closely related. Thus, the results from the present experiments are discussed below in terms of turbulence production, redistribution of turbulence energy and propagation of turbulence across the flow.

6.1. Turbulence production

An imposed pulsation of flow rate can be viewed as a series of small perturbations which are imposed successively on a steady flow. Each flow perturbation will be felt first at the wall due to the no-slip condition and will cause a change in the velocity field very near the wall, which will diffuse away from it. The turbulence in the flow will remain unaffected by each perturbation of flow rate until the change in the mean velocity field is felt in the region where turbulence production mainly occurs. Then additional turbulence will be produced in response to the change in the velocity field. It can be argued that the ratio of the distance that the disturbance to the velocity field diffuses away from the wall within any one pulsation cycle, i.e. the Stokes layer thickness, l_s $(=\sqrt{2\nu/\omega})$, to the distance from the wall to the location where turbulence production is concentrated ($y^+ \approx 10$), is likely to be important in characterising the response of turbulence to flow rate perturbations. Consistent with this, Tardu et al. [29] found that the critical value of l_s^+ was about 10 for the turbulence present in a pulsating flow to be significantly affected by an imposed pulsation of flow rate in a channel. In some other studies the related parameter ω^+ $(= 2/l_s^{+2})$, sometimes referred to as the inner scale Strouhal number, has been used instead of l_s^+ to correlate such experimental data. Both parameters l_s^+ and ω^+ are based on the idea of interaction between turbulence production and the Stokes layer. Therefore they are particularly suitable when the focus is on turbulence behaviour near the wall or on the wall shear stress. As we have seen earlier, Ramaprian and Tu [17] and Scotti and Piomelli [38] took the idea further by introducing the concept of the turbulent penetration depth l_t so as to be able describe processes beyond the near-wall region into the buffer layer region. l_t^+ is simply a function of l_s^+.

The dynamic processes involved in turbulence production just described can be seen in the response exhibited in the present study by the rms velocity fluctuation u' in the near wall region, even though measurements are only available beyond $y^+ \approx 12$. It can be seen from Fig. 5(a) that, for the lower frequency cases, where l_s^+ is greater than 11 (experiments T6, T10 and T20), the distribution of amplitude of the modulation of rms fluctuation of axial velocity u' near the wall remained basically unchanged as the frequency was varied and was in each case quite similar to that for quasi-steady flows obtained from the series of steady state measurements. However, as the frequency of pulsation was increased so that l_s^+ became less than about 10, (experiments T2 and T3), the amplitude of the modulation of u' started to reduce with increase of the pulsation frequency. Under such conditions, the pulsation time period was so short that the unsteadiness imposed on the mean flow could not be transmitted within any one cycle from the wall to the region where turbulence production is significant and, therefore, the production of additional turbulence is attenuated. The above ideas are illustrated in Fig. 10 where the normalised amplitudes of the modulation of the rms velocities u' and v' at

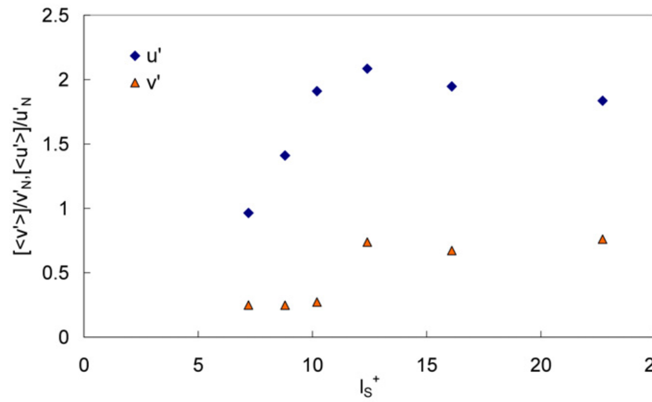

Fig. 10. Normalised amplitude of the modulation of the rms fluctuating velocities at $y^+ = 12$.

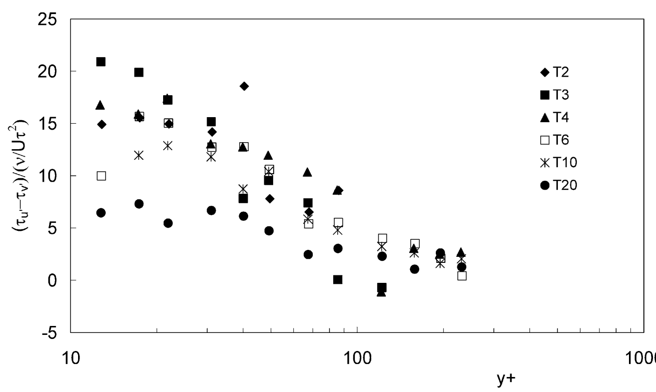

Fig. 11. Difference between the delays in the axial and radial components of rms fluctuating velocity.

$y^+ = 12$ are plotted against l_s^+ for the various cases with a mean Reynolds number of 7000. Similar behaviour can be seen in the results of Tu and Ramaprian [16].

6.2. Turbulence energy redistribution between the components

An interesting aspect of the response of turbulence near a wall to a flow rate excursion is associated with the fact that turbulence production is initially only manifested as a change in the axial component of turbulent fluctuation u'. The other two components v' and w' are modified through redistribution of turbulent kinetic energy by the action of pressure which causes transfers from the axial to the transverse and circumferential components. Therefore, additional delays occur in the responses of v' and w'. This is demonstrated in Fig. 11 in the case of the transverse component v' where the time lag between the response of the u' and v', normalised using the time scale ν/u_τ^2, is shown. The time lag is the highest at the first measurement point ($y^+ = 12$) and reduces further away from the wall, becoming practically negligible in the core region ($y^+ > 80$). Results obtained by Brereton and Reynolds [37] showed a similar trend. With more detailed measurements near the wall, they were able to show that the peak lag occurs at around $y^+ = 8$. The values of normalised delay in the measurements of Brereton and Reynolds were higher than in the present study which could have been a consequence of the different range of conditions covered and/or the different flow configuration used.

As a result of the further time scale associated with turbulent kinetic energy redistribution in the near-wall region, an attenuation of the amplitude of the modulation of v' and w' can be seen even in a relatively slow transient, for which no attenuation can be seen in the case of u'. For example, a small yet clear attenuation can be identified in the v' modulation near the wall even in experiment T10 ($l_s^+ \approx 16$), see Fig. 5. This kind of attenuation is not evident in the case of u' until the period of pulsation is reduced to around 4 seconds (experiment T4). Now, because the u' and v' modulations are always out of phase, and the v' modulation is more severely attenuated than is the u' modulation, the degree of turbulence anisotropy can be significantly modified in pulsating flow. Clearly, this presents a challenge to turbulence modellers.

6.3. *Turbulence propagation across the core flow*

The further stage to be considered in the response of turbulence to an imposed pulsation of flow rate is the propagation of new turbulence produced in the near-wall region into and across the core flow. Associated with this there is a further time lag in the modulation of u' and v', which increases gradually with distance from the wall region across the flow. It can be seen from Fig. 8 that this varies in a linear manner over most of the flow, implying a constant speed of turbulence propagation, except near the axis of the pipe where the rate of increase of the time lag does reduce. The propagation speed remains unchanged with increase of frequency (i.e., the radial distributions on the figure are parallel), but reduces with increase of mean flow rate. The latter can be inferred to from the fact that the non-dimensional delay $[\tau/(R/u_\tau)]$ is independent of the mean Reynolds number, which implies that the propagation speed is proportional to the friction velocity u_τ. These observations are consistent with arguments presented in Section 1 based on ideas from Scotti and Piomelli [38] which also led to the conclusion that the shear waves propagate through the turbulent core of a pulsating pipe flow at a speed almost equal to u_τ. It follows from the preceding discussion that the value of the non-dimensional outer scaling parameter $T^*(= Tu_\tau/R)$ in relation to unity should provide an indication as whether turbulence in the core region is 'frozen' or not. Applying this criterion to the present experiments for $Re = 7000$, we found that the time period of the flow pulsation should be less than about 4 seconds for turbulence in the core to be frozen. This is closely consistent with what was observed.

From the foregoing discussion, it is apparent that using 'time delay' rather than 'phase shift' in the evaluation of results from pulsating flow experiments has some advantages. The absolute time delay is mainly dependent on the mean flow rate and remains quite similar for pulsating flows with various frequencies but constant mean flow rate. On the other hand, if phase shift is used as a parameter, even when the mean flow rate is fixed (i.e., the actual process of propagation remains unchanged), the phase shift will still change as the frequency of the imposed flow pulsation is varied (as was seen in Fig. 7). Thus, working in terms of phase shift rather than time delay could obscure what is really happening. The time lag of turbulence response in pulsating flows was examined in Binder et al. [28] and Scotti and Piomelli [38]. In both studies the time lags were normalise using a parameter based on inner rather than outer scales. As a result the trends exhibited vary with mean flow rate.

It is helpful to have some feel for the relative magnitudes of the time scales associated with the various processes involved in the response of turbulence in pulsating flows. For this purpose, we assume that the time scales associated with turbulence production, redistribution of energy between its components and radial propagation of turbulence response across the flow can be approximately represented by the delays in u' at $y^+ = 12$, the difference between the delays in u' and v' at that position, and the difference between the delays of u' at the centre and $y^+ = 12$, respectively. The normalised delays involved in the three processes can then be obtained from Fig. 8. For Re = 7000, the delays in real terms are found to be about, 0.5 s, 1 s and up to 4 s, respectively. The significance of these various processes on the response of turbulence in a pulsating flow depends on the frequency of the pulsation and whether the main interest is in what is happening within the wall region or in the core region. For pulsations of higher frequency, such as, cases T2 and T3 in the present study, the effect of the pulsation is restricted to the near-wall region, and the mean flow and turbulence are frozen over most of the core flow. Under such conditions, radial propagation of turbulence response ceases to play any role. The pulsating flow is characterised by the degree of the attenuation of the modulation of the turbulence production near the wall. The higher the frequency the more severely is the response of turbulence attenuated by the pulsation. It is apparent that, for such conditions, non-dimensional correlating parameters, such as l_S^+ or ω^+, are appropriate. When the frequency of the flow pulsation is lower, the reduction in the modulation of near-wall turbulence response will be insignificant (i.e., turbulence production will not be markedly attenuated). Under these conditions, the radial propagation of the near-wall response outwards to the centre of the pipe plays a dominant role in determining the overall flow behaviour. Therefore non-dimensional correlating parameters associated with turbulence propagation, such as T^* or $\omega D/u_\tau$, are appropriate for characterising the overall flow behaviour.

7. Conclusions

The results of this study of turbulent pulsating flow show that the variation with frequency of the amplitude of velocity modulation exhibits a non-monotonic but consistent pattern. In the case of the higher frequencies covered, the flow in the core region exhibits a 'frozen' slug-like behaviour, the amplitude of the velocity modulation being constant in that region. With reduction of pulsation frequency, the extent of this region reduces until eventually 'freezing' no longer occurs. In fast pulsating flows, the maximum amplitude of the velocity modulation occurs at a location near to the wall. It moves away from the wall as the frequency of the pulsation reduces and for pulsations of very low frequencies, the maximum amplitude occurs at the centre of the pipe. The responses of the axial and radial components of rms fluctuating velocity are quite similar in the core region of the flow but are different in the wall region, where the latter exhibits a bigger delay than the former. This difference is associated with turbulence energy redistribution from the axial component to the other components. In the core region, the amplitude of modulation of both the axial and radial components of RMS turbulent fluctuation reduces with the increase in the frequency of the flow pulsation, eventually becoming zero as the turbulence field in that region becomes 'frozen'. The response of turbulence to an imposed pulsation of flow rate initially occurs in the wall region and then propagates into and across the core. Thus there is an additional time delay in the response of the turbulent fluctuation in the core region, which grows with the distance from the wall. It remains more or less the same irrespective of the frequency of the flow pulsation but decreases with increase of mean flow rate. Absolute delay time has some advantage over phase shift for characterising the delay in the response of turbulence at various radial positions. The similarity parameter $\omega D/u_\tau$ or the related one $T^*(= u_\tau T/R)$, are both appropriate for correlating the data on the flow and turbulence in the core region. However the parameters l_s^+, or ω^+ should be used when consideration is focused on the near-wall response, especially for pulsations of high frequency.

References

[1] S. Uchida, The pulsating viscous flow superimposed on the steady laminar motion of incompressible fluid in a circular pipe, Z. Angew. Math. Phys. 7 (1956) 377.

[2] G.G. Stokes, On the effect of the internal friction of fluids on the motion of pendulums, Trans. Cambridge Philos. Soc. 9 (8) (1850);
Reprinted in G.G. Stokes, Mathematical and Physical Papers, Cambridge University Press, Cambridge, 1901.
[3] G.J. Brereton, R.R. Mankbadi, Review of recent advances in the study of unsteady turbulent internal flows, Appl. Mech. Rev. 48 (1995) 189–212.
[4] M.Y. Gundogdu, M.O. Carprilioglu, Present state of art on pulsating flow theory (part 2: turbulent flow regimes), JSME Int. J. 42 (1999) 398–410.
[5] A.K.M.F. Hussain, W.C. Reynolds, The mechanics of an organised wave in turbulent shear flow, J. Fluid Mech. 41 (1970) 241.
[6] A.K.M.F. Hussain, W.C. Reynolds, The mechanics of an organised wave in a turbulent shear flow, J. Fluid Mech. 5 (1972) 622.
[7] C. Ahrens, D. Ronneberger, Luftschall damepfung in turbulent durchstromten schallharton Rohren bei verschidenen Wandrauhigkeiten, Acoustica 25 (1971) 150–157.
[8] C. Ahrens, Wechselwirkung zwischen zahigeitswellen und wandnaher Turbulenz in Wasser mit ohue Zusatz einer reibungsuermisdaruden Substanz, PhD Dissertation Math. Nat. Fakultat, Universitat, Gottinger, 1973.
[9] M. Archarya, W.C. Reynolds, Measurements and predictions of a fully developed turbulent channel flow with imposed controlled oscillations, Dept. Mech. Eng. Stanford Univ. Report TF-8, 1975.
[10] D. Ronneberger, Genaue Messung des Schall damp fung und der Phas geschwinditeit in durchstromten Rohren im Himblick auf die Wechselwirkung zwischen Schall and Turbulenz, Habilitationschrift Math. Nat. Fak Univ. Gotttingen, 1975.
[11] D. Ronneberger, C.D. Aherens, Wall shear stress caused by small amplitude perturbations of turbulent boundary-layer flows: an experimental investigation, J. Fluid Mech. 83 (1977) 433–464.
[12] J.H. Gerrard, An experimental investigation of pulsating turbulent water flow in a tube, J. Fluid Mech. 46 (1971) 43–64.
[13] T. Mizushima, T. Maruyama, Y. Shiozaki, Pulsating turbulent flow in a tube, J. Chem. Eng. Japan 6 (1973) 487–494.
[14] T. Mizushima, T. Maruyama, H. Hirasawa, Structure of the turbulence in pulsating pipe flows, J. Chem. Eng. Japan 8 (3) (1975) 210–216.
[15] B.R. Ramaprian, S.W. Tu, An experimental study of oscillatory pipe flow at transitional Reynolds numbers, J. Fluid Mech. 100 (1980) 513–544.
[16] S.W. Tu, B.R. Ramaprian, Fully developed periodic turbulent pipe flow. Part 1. Main experimental results and comparison with predictions, J. Fluid Mech. 137 (1983) 31–58.
[17] B.R. Ramaprian, S.W. Tu, Fully developed periodic turbulent pipe flow. Part 2. The detailed structure of the flow, J. Fluid Mech. 137 (1983) 59–81.
[18] L. Shemer, I. Wygnanski, On the pulsating flow in a pipe, in: 3rd Symposium on Turbulent Shear Flows, Proceedings, University of California, Davis, 1981, pp. 8.13–8.18.
[19] L. Shemer, E. Kit, An experimental investigation of the quasi-steady turbulent pulsating flow in a pipe, Phys. Fluids 27 (1) (1984) 72–76.
[20] L. Shemer, I. Wygnanski, E. Kit, Pulsating flow in a pipe, J. Fluid Mech. 153 (1985) 313–337.
[21] S. Burnel, J.C. Raelison, J.M. Thomas, Radial distribution of the Reynolds stress in a turbulent pulsating flow in a pipe flow, in: Engineering Turbulence Modelling and Experiments, Proceedings of the International Symposium on Engineering Turbulence Modelling and Measurements, Dubrovnik, Yugoslavia, 1990.
[22] Z. Mao, T.J. Hanratty, Studies of wall shear stress in a turbulent pulsating pipe flow, J. Fluid Mech. 170 (1986) 545–564.
[23] D.S. Finnicum, T.J. Hanratty, Influence of imposed flow oscillations on turbulence, Phys. Chem. Hydrodyn. 10 (1988) 585.
[24] Z. Mao, T.J. Hanratty, Measurement of wall shear rate in large amplitude unsteady reversing flows, Exp. Fluids 12 (1992) 342.
[25] Z. Mao, T.J. Hanratty, Influence of large amplitude oscillations on turbulent drag, ATChE. J. 40 (1994) 1601.
[26] J.L. Hwang, G.J. Brereton, Turbulence in high frequency periodic fully developed pipe flow, in: F. Durst, R. Friedrich, B.E. Launder, F.W. Schmidt, U. Schuman, J.H. Whitelaw (Eds.), Turbulent Shear Flow 8, Selected Papers from the Eighth Internaitonal Symposium on Turbulent Shear Flows, Munich, Germany, 9th–11th September 1991, Springer, Berlin, 1993.
[27] G. Binder, J.L. Kueny, Measurements of the periodic velocity oscillations near the wall in unsteady turbulent channel flow, in: Q. Bradbury, Q. Durst, Q. Launder, Q. Schmidt, Q. Whitelaw (Eds.), Turbulent Shear Flow 3, Springer-Verlag, 1981, pp. 6–17.
[28] G. Binder, S. Tardu, R.F. Blackwelder, J.L. Kueny, Large amplitude periodic oscillations in the wall region of a turbulent channel flow, in: Fifth Symposium on turbulent Shear Flows, Cornell University, Ithaca, New York, 1985.
[29] S. Tardu, G. Binder, R.F. Blackwelder, Turbulent channel flow with large-amplitude velocity oscillations, J. Fluid Mech. 267 (1994) 109–151.
[30] S.F. Tardu, G. Binder, Wall shear stress modulation in unsteady turbulent channel flow with high imposed frequencies, Phys. Fluids A 5 (1993) 2028–2037.
[31] G. Binder, J. Tardu, P. Vezin, Cyclic modulation of Reynolds stresses and length scales in pulsed turbulent channel flow, Proc Roy. Soc. London Ser. A 451 (1995) 121.
[32] S. Tardu, G. Binder, Reaction of bursting to an oscillating homogeneous pressure gradient, Eur. J. Mech. B/Fluids 16 (1997) 89.
[33] S.F. Tardu, P. da Costa, Experiments and modelling of an unsteady turbulent channel flow, AIAA J. 43 (2005) 140–148.
[34] S.K.F. Karlsson, An unsteady turbulent boundary layer, J. Fluid Mech. 5 (1959) 622–636.
[35] J. Cousteix, J. Javelle, R. Houdeville, Influence of Strouhal Number on the structure of a flat plate turbulent boundary layer, in: 3rd Symposium on Turbulent Shear Flows, University of California, Davis, USA, 1981.
[36] G.J. Brereton, W.C. Reynolds, R. Jayaraman, Response of a turbulent boundary layer to sinusoidal free-stream unsteadiness, J. Fluid Mech. 221 (1990) 131–159.
[37] G.J. Brereton, W.C. Reynolds, Dynamic response of boundary-layer turbulence to oscillatory shear, Phys. Fluids A 3 (1991) 178–187.
[38] A. Scotti, Piomelli, Numerical simulation of pulsating turbulent channel flow, Phys. Fluids 13 (2001) 1367–1384.
[39] S. He, J.D. Jackson, A study of turbulence under conditions of transient flow in a pipe, J. Fluid Mech. 408 (2000) 1–38.